Catalysis Letters 21 (1993) 113–122

Methane oxidative coupling over fluoro-oxide catalysts ☆

Xiaoping Zhou, Weide Zhang, Huilin Wan and Khirui Tsai

Department of Chemistry, Xiamen University, Xiamen 361005, PR China

Received 27 January 1993; accepted 12 May 1993

LaF_3 modified ZrO_2, CeO_2 and ThO_2 catalysts for the oxidative coupling of methane indicate that ZrO_2/LaF_3, CeO_2/LaF_3 and ThO_2/LaF_3 catalysts have high activity and high selectivity at low temperature. In the temperature region 480–650°C, the methane conversion is 24.38–30.8% and the $C_2^=$ selectivity is 40–55.38%. The characterization of oxygen species on the catalysts indicates that, because of the modification of LaF_3 to ZrO_2, CeO_2 and ThO_2, it is favourable for the activation of O_2.

Keywords: Fluoro-oxide catalysts; modification; active oxygen species; methane oxidative coupling

1. Introduction

Since in 1982 Keller and Bhasin reported their work on methane oxidative coupling [1], almost all of the catalysts developed were oxide catalysts or alkali metal ion and Cl^- promoted oxide catalysts [2–5]. These catalysts must be operated at high temperature (about 750°C). This led to gas phase nonselective oxidation, and the loss of alkali metal ion and Cl^- caused the decrease in activity and selectivity of the catalysts. In order to overcome this problem, we developed a series of fluoro-oxide catalysts which could be operated at 480–650°C. They had good mechanical strength and catalytic stability.

2. Experiment

The catalysts were prepared separately from the following reagents: FA, LaF_3/ZrO_2 (2 : 1); FB, LaF_3/CeO_2 (2 : 1); FC, LaF_3/CeO_2 (4 : 1); FD, LaF_3/ThO_2 (2 : 1); FE, LaF_3/ThO_2 (4 : 1) (all ratios are in mol). The mixtures were crushed

---

☆ Patent application No. CN 92105258.8 inventors: Xiaoping Zhou, Huilin Wan and K.R. Tsai.

and then stirred with deionized water to paste. The pastes were dried at 100°C for 1 h, then calcined at 900°C for 6 h, and then crushed to 0.22–0.45 mm particle size. In this way, the catalysts FA, FB, FC, FD and FE were prepared.

Catalytic reaction was carried out in a quartz tube fixed bed reactor. 0.2 ml of catalyst was used. The reactant feed rate ($CH_4 : O_2 = 3 : 1$) was 50 ml/min. The product analysis was carried out on a 102GD gas chromatograph.

The XRD measurements of the fresh catalysts were carried out by using a Rigaku Rotaflex D/Max-C system with Cu K_α radiation.

The XPS measurements were carried out on an ESCALAB MKII system with Al K_α radiation ($h\nu = 1486.6$ eV) at room temperature and a pressure 1×10^{-9} Pa. The samples were treated in a quartz tube reactor in H_2 stream at 900°C for 30 min, then treated in He stream at 900°C for 30 min, cooled to room temperature in He stream, adsorbed pure oxygen (O_2) at room temperature, passed through with He, and then the samples were sealed in glass tubes in He stream respectively. The tubes of samples adsorbed with oxygen were broken in the sample treatment cavity of the XPS system. The samples were not exposed to air in the treatment procedure and during measurement of O 1s XPS. The O 1s XPS spectra were recorded at room temperature.

The Raman spectra were recorded by using a Jobin Yvon U-1000 Raman spectrometer. The treatment used in Raman characterization, was as follows: The catalyst sample was treated in H_2 stream at 900°C for 30 min, then treated in He stream at 900°C for 30 min, cooled to room temperature, and part of the sample was sealed in a glass tube in He stream, thus obtaining a no O_2 adsorbed sample (background sample). The rest of the sample was passed through with O_2 at room temperature, and then passed through with He at room temperature and sealed in a glass tube, thus obtaining an O_2 adsorbed sample. The background samples and the O_2 adsorbed samples were not exposed to air during the treatment procedure and Raman measurement.

The sample used in the TPD measurement was treated in a quartz desorption reactor in H_2 stream at 900°C for 30 min, cooled to room temperature in He stream, and then passed through with O_2 at room temperature. Helium gas was used as carrier gas. The desorption was carried out at a temperature increasing rate of 15°C/min.

3. Results and discussion

The data of table 1 were obtained after 24 h operating of the catalysts, and in the course of 200 h, the CH_4 conversions and C_2 selectivities did not change with time on stream. The total carbon material balance is about 98% based on CO, CO_2, C_2H_4 and C_2H_6. A trace amount of CH_2O was formed (in H_2O about 1%). In the first 24 h, the fluorine was found losing.

From the result of table 1, we know that on CeO_2, methane was almost comple-

Table 1
The performance of catalysts

Cat.	React. T (°C)	Selectivity (%)			Conver. of CH_4 (%)	Select. of C_2 (%)	C_2 yield (%)
		CO	CO_2	$C_2^=/C_2$			
ZrO_2	700	13.9	70.0	0.94	25.96	16.06	4.17
	600	13.4	72.9	0.90	23.0	13.7	3.15
	500	no activity					
CeO_2	650	10.1	87.0	0	20.7	3.9	0.8
	500	13.7	84.4	0	21.1	1.9	0.4
ThO_2	850	14.0	54.0	1.67	24.0	32.0	7.7
	800	no activity					
LaF_3	650				6.75	12.06	0.81
FA	650	0	47.8	1.42	27.1	52.2	14.1
FB	550	0	49.6	1.07	28.82	50.35	14.51
	500	0	47.9	1.01	28.17	52.14	14.70
FC	600	2.2	49.7	1.07	28.88	48.15	13.91
	500	0	44.6	0.90	24.38	55.38	13.45
FD	550	4.7	50.9	1.05	29.63	44.51	13.19
	500	4.5	53.3	0.93	28.52	40.75	11.62
FE	500	13.1	41.4	0.98	30.8	45.6	14.04
	480	11.0	43.9	0.94	28.5	45.1	12.80

tely combusted. Over ZrO_2 catalyst, the C_2 selectivity was better than over CeO_2. The C_2 selectivity on ThO_2 was the highest among CeO_2, ZrO_2 and ThO_2, but the reaction must be carried out at high temperature. The CH_4 conversion and C_2 selectivity were low over LaF_3. After the modification of LaF_3 to ZrO_2, CeO_2 and ThO_2, the oxidative coupling of methane could be carried out at 480–650°C, the CH_4 conversion and C_2 selectivity increased apparently. Over catalyst LaF_3/ZrO_2 (2 : 1), the CH_4 conversion increased to 27% (23–26% over ZrO_2), and the C_2 selectivity increased from 14–16% to 52%. Over catalysts LaF_3/CeO_2 (2 : 1) and LaF_3/CeO_2 (4 : 1), the CH_4 conversion was 8% higher than over CeO_2, and the C_2 selectivity increased about 12 times comparing to that over CeO_2. Over LaF_3/ThO_2 (2 : 1), and LaF_3/ThO_2 (4 : 1) catalysts which contained ThO_2, the CH_4 conversion and C_2 selectivity also increased remarkably. From table 1, we can find that the CH_4 conversion and C_2 selectivity of LaF_3/CeO_2 (2 : 1) and LaF_3/CeO_2 (4 : 1) were better than that of LaF_3/ZrO_2 (2 : 1), but that of LaF_3/ZrO_2 (2 : 1) was better than that of LaF_3/ThO_2 (2 : 1) and LaF_3/ThO_2 (4 : 1). The difference of catalytic properties of these catalysts may be the result from their different microstructure, different oxygen activation ability and different kinds of active oxygen species distribution. From table 1, we can also find that the catalytic properties of LaF_3/CeO_2 (2 : 1) and LaF_3/CeO_2 (4 : 1) or LaF_3/ThO_2 (2 : 1) and LaF_3/ThO_2 (4 : 1) do not change apparently with the content of CeO_2 or ThO_2 in the catalysts.

This indicated that in a range of CeO_2 or ThO_2 content, maybe the sorts and concentration of oxygen species on the catalyst surface were similar.

XRD analysis indicated that, in catalyst LaF_3/ZrO_2 (2 : 1) the main phases are hexagonal LaF_3, monoclinic ZrO_2, tetragonal LaOF and rhombohedral LaOF. In LaF_3/CeO_2 (2 : 1) the main phases are monoclinic LaF_3, cubic CeO_2 and tetragonal LaOF. In LaF_3/CeO_2 (4 : 1), the main phases are hexagonal LaF_3, cubic CeO_2 and tetragonal LaOF and a little hexagonal LaF_3. In LaF_3/ThO_2 (4 : 1), the main phases are cubic ThO_2, monoclinic LaF_3 and tetragonal LaOF. The above results indicated that, in the process of the preparation of catalysts, $O^{2-} \leftrightarrow F^-$ exchange happened between solid lattices. This kind of exchange (one O^{2-} can substitute two F^-) would form anion vacancies. It is favourable for the activation of O_2, making the catalysts have high activity at relatively low temperature.

XPS characterization of oxygen species on catalysts. Fig. 1 shows XPS spectra of O 1s electron binding energy. On O_2 adsorbed ZrO_2, CeO_2 and ThO_2, the binding energies of O 1s were 529.5, 529.1 and 529.2 eV respectively. The oxygen species on ZrO_2, CeO_2 and ThO_2 may be O^{2-} [6].

Fig. 2 shows the XPS spectra of oxygen species on catalysts LaF_3/ZrO_2 (2 : 1), LaF_3/CeO_2 (2 : 1) and LaF_3/ThO_2 (2 : 1). It can be found that after the modification of LaF_3, the O 1s peaks became broad. From the resolution of these energy peaks, we inferred that there were three kinds of oxygen species on LaF_3/ZrO_2 (2 : 1) with binding energies 528.2, 530.0 and 531.6 eV respectively. On LaF_3/CeO_2

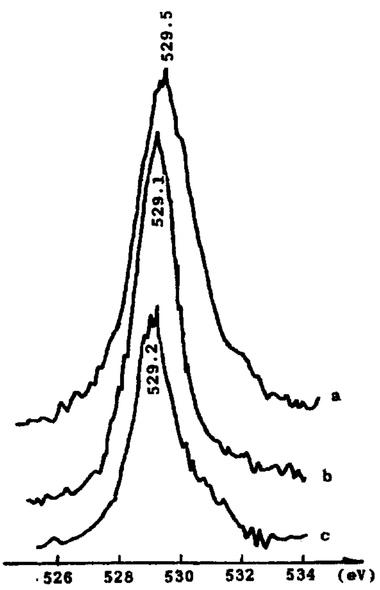

Fig. 1. O 1s XPS spectra of oxygen adsorbed (a) ZrO_2, (b) CeO_2, (c) ThO_2 (recorded at room temperature).

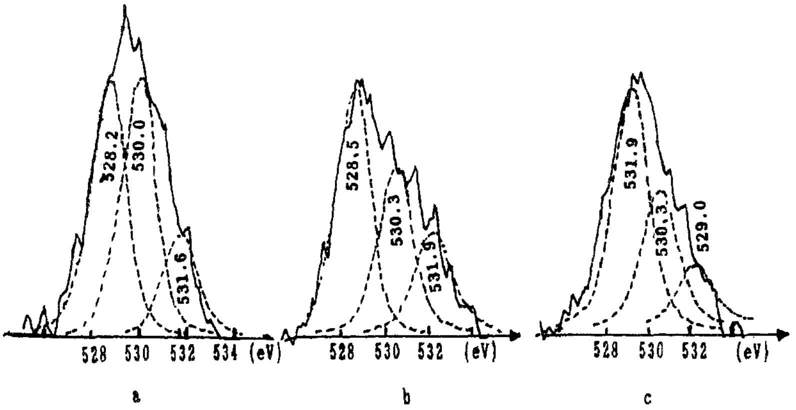

Fig. 2. O 1s XPS spectra of oxygen adsorbed (a) LaF_3/ZrO_2 (2 : 1), (b) LaF_3/CeO_2 (2 : 1), (c) LaF_3/ThO_2 (2 : 1).

(2 : 1), there were three kinds of oxygen species with binding energies 528.5, 530.3 and 531.9 eV respectively. On LaF_3/ThO_2 (2 : 1), there were also three kinds of oxygen species with binding energies 529.0, 530.3 and 531.9 eV respectively. The above peaks with binding energies at 528.2, 528.5 and 529.0 eV may be the peaks of O^{2-} 1s electron binding energy [6], while the peaks at 530.0 and 530.3 eV may be energy peaks of O^{2-}, which are located in other chemical environments. The peaks at 531.6 and 531.9 eV may be belong to the active oxygen species O^-, O_2^{2-} and O_2^- [6], and oxygen in carbonate. But the amount of carbonate might be small, because under our sample treatment condition carbonate is unstable. Under our sample treatment condition, hydroxide ions could not exist on catalysts. In our following Raman measurement, we did not find the characteristic bands of CO_3^{2-}. So it is reasonable to assign the high binding energy peaks of oxygen species in fig. 2 to active oxygen species O^-, O_2^{2-}, O_2^- and the oxygen in carbonate.

The above O 1s XPS results elucidated that, after the modification of LaF_3 to ZrO_2, CeO_2 and ThO_2, the ability of catalysts for the activation of O_2 increased.

Raman characterization of active oxygen species on catalysts. Fig. 3 shows Raman spectra of catalysts. On no O_2 adsorbed LaF_3/ZrO_2 (2 : 1), LaF_3/CeO_2 (2 : 1) and LaF_3/CeO_2 (4 : 1), in the region of 600–1500 cm^{-1}, no bands were observed. For no O_2 adsorbed LaF_3/ThO_2 (2 : 1), the bands are 938, 1026, 1062, 1124, 1366 cm^{-1} (broad band). On no O_2 adsorbed LaF_3/ThO_2 (4 : 1), the bands are 894, 938, 1032, 1076, 1138, 1316 and 1374 cm^{-1}. For no O_2 adsorbed ThO_2 and LaF_3 in the region of 600–1500 cm^{-1}, no band was observed.

On O_2 adsorbed LaF_3/ZrO_2 (2 : 1), 622, 646 and 858 to 934 cm^{-1} bands were observed. They might arise from O_2^{2-} species, which adsorbed on different chemical environments [7–10]. However, the wavenumbers 622 and 646 cm^{-1} are much lower than 850 cm^{-1} which was observed on O_2 adsorbed metal surface, which was assigned to O_2^{2-} ions [11,12]. But the two Raman bands did not appear on back-

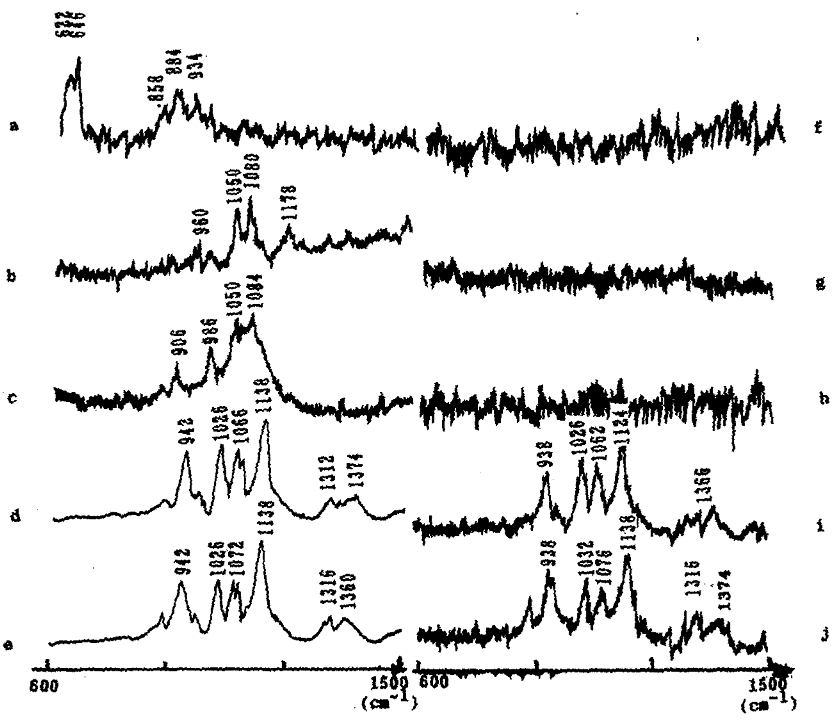

Fig. 3. The Raman spectra of oxygen species on catalysts (amplification factor is 1 × 10^3). Oxygen adsorbed samples: (a) LaF_3/ZrO_2 (2 : 1), (b) LaF_3/CeO_2 (2 : 1), (c) LaF_3/CeO_2 (4 : 1), (d) LaF_3/ThO_2 (2 : 1), (e) LaF_3/ThO_2 (4 : 1). Background samples (treatment condition is described in experimental section): (f) LaF_3/ZrO_2 (2 : 1), (g) LaF_3/CeO_2 (2 : 1), (h) LaF_3/CeO_2 (4 : 1), (i) LaF_3/ThO_2 (2 : 1), (j) LaF_3/ThO_2 (4 : 1).

ground sample LaF_3/ZrO_2 (2 : 1), and our other background samples, for instance CaF_2/ZrO_2 (2 : 1), BaF_2/ZrO_2 (2 : 1) and $BaF_2/LaF_3/ZrO_2$ (1 : 1 : 1). When O_2 was adsorbed on these background samples, the bands at 622 and 646 cm^{-1} appeared (which will be published in our other paper). In the Raman study, in the wavenumber region of 200–600 cm^{-1}, we observed the characteristic band at 474 cm^{-1} on the above catalysts both under oxygen adsorbing condition and their background. This band was also observed on background ZrO_2 (treated according to the method which was described in section 2). The band at 474 cm^{-1} might arise from Zr–O–Zr or Zr=O vibration, which are close to the band found in CeO_2 and assigned to Ce^{4+}–O–Ce^{4+} bond vibration by Graham et al. [13]. The bands at 622 and 646 cm^{-1} arose from O_2 adsorption, and might arise from dioxygen species on catalyst LaF_3/ZrO_2 (2 : 1). So we tried to assign the two bands to O_2^{2-} ions. The verification work is in progress. For O_2 adsorbed LaF_3 /CeO_2 (2 : 1), 960, 1050, 1080 and 1178 cm^{-1} bands were observed. These bands may belong to O_2^- species, which are located in different adsorption centers [14–16]. LaF_3/CeO_2 (4 : 1) and LaF_3/CeO_2 (2 : 1) have the same resource substance LaF_3 and CeO_2, but the CeO_2

content in LaF_3/CeO_2 (4 : 1) was only half of that in LaF_3/CeO_2 (2 : 1). On O_2 adsorbed LaF_3/CeO_2 (4 : 1), besides the bands between 1050 and 1084 cm^{-1}, which were observed on LaF_3/CeO_2 (2 : 1), there were still two new bands at 906 and 986 cm^{-1}, and the band at 1178 cm^{-1} observed on LaF_3/CeO_2 (2 : 1) was not found on LaF_3/CeO_2 (4 : 1). The peaks at 906 and 986 cm^{-1} may be the bands of oxygen species intermediate between O_2^{2-} and O_2^- species [17–20] or of O_2^{2-}. On O_2 adsorbed LaF_3/ThO_2 (2 : 1), the band shape and position are similar to those of no O_2 adsorbed LaF_3/ThO_2 (2 : 1), but the strength of bands on O_2 adsorbed LaF_3/ThO_2 (2 : 1) was much stronger than those of no O_2 adsorbed LaF_3/ThO_2 (2 : 1). The case of O_2 adsorbed LaF_3/ThO_2 (4 : 1) was similar to that of LaF_3/ThO_2 (2 : 1). These bands observed on LaF_3/ThO_2 (2 : 1) and LaF_3/ThO_2 (4 : 1) might arise from certain lattice vibrations and active oxygen species. Therefore in our following TPD characterization of oxygen, the desorption peak from 35 to 270°C might be assigned to O_2^- ions, and the desorption peak from 342 to 718°C might be assigned to O_2^{2-} species [21,22]. From fig. 3, we can find that O_2^-, O_2^{2-} ions on LaF_3/ThO_2 (2 : 1) and LaF_3/ThO_2 (4 : 1) were much more stable than those of LaF_3/ZrO_2 (2 : 1), LaF_3/CeO_2 (2 : 1) and LaF_3/CeO_2 (4 : 1), and the peaks under 1000 cm^{-1} were stronger than those of LaF_3/ZrO_2 (2 : 1), LaF_3/CeO_2 (2 : 1) and LaF_3/CeO_2 (4 : 1). This means O_2^{2-} species concentrations of LaF_3/ThO_2 (2 : 1) and LaF_3/ThO_2 (4 : 1) were much higher than those of corresponding species on LaF_3/ZrO_2 (2 : 1), LaF_3/CeO_2 (2 : 1) and LaF_3/CeO_2 (4 : 1).

From the Raman spectra of the catalysts, we inferred that the main active oxygen species on LaF_3/ZrO_2 (2 : 1) might be O_2^{2-} ions, the main active oxygen species on LaF_3/CeO_2 (2 : 1) and LaF_3/CeO_2 (4 : 1) might be O_2^- ions and a little amount of O_2^{2-} ions. But on LaF_3/ThO_2 (2 : 1) and LaF_3/ThO_2 (4 : 1), besides a large amount of O_2^- and O_2^{2-}, maybe there were a large amount of intermediate oxygen species. The Raman results also elucidated that, after the modification of LaF_3 to ZrO_2, CeO_2 and ThO_2 the oxygen activation ability of catalysts increased. This is in agreement with the XPS result.

Oxygen TPD of catalysts. Fig. 4a is the oxygen TPD curve of catalyst LaF_3/ZrO_2 (2 : 1). There are four peaks from 60 to 860°C. Their temperature regions are 63–274°C, 274–500°C, 500–718°C, and from 718°C to even higher temperature. In the Raman measurement, no bands of O_2^- ions were observed, so the peaks from 63 to 860°C may be the desorption of O_2^{2-} and O^- ions, which are located in different chemical environments. The desorption of 63 to 274°C might be the weakly adsorbed O_2^{2-}, while the strong band from 274 to 500°C might be the desorption of tightly adsorbed O_2^{2-} ions, which might correspond to the oxygen species of which the Raman bands are at 622 to 646 cm^{-1}. The desorption bands above 500°C, might be the desorption of O^- or part of O^{2-} [22].

Fig. 4b shows the oxygen TPD spectrum of LaF_3/CeO_2 (2 : 1). There is only one peak from 38 to 800°C. Its temperature region is 38–133°C. It might be the desorption of O_2^- ions [22,23].

Fig. 4c shows the oxygen TPD spectrum of LaF_3/CeO_2 (4 : 1). On this catalyst,

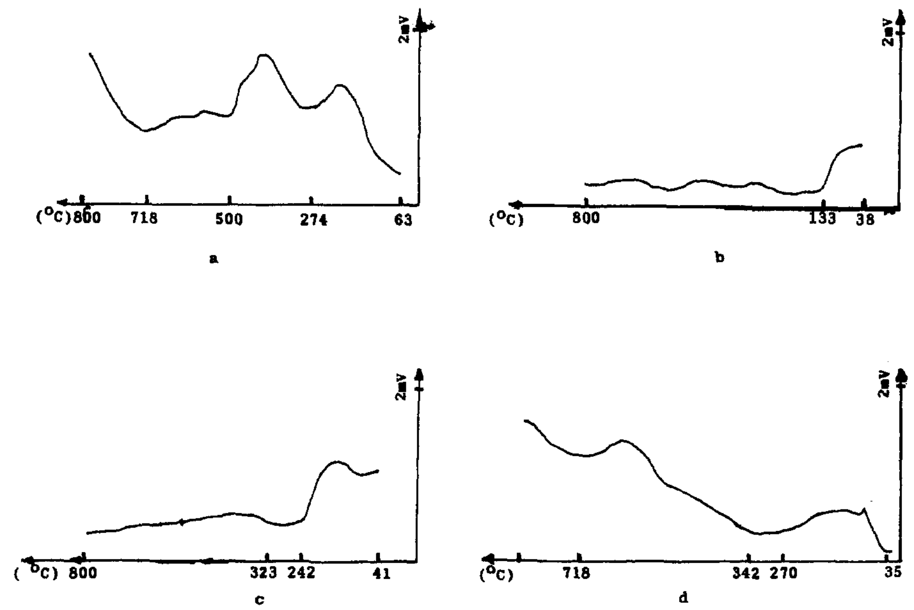

Fig. 4. The oxygen TPD spectra of catalysts (a) LaF_3/ZrO_2 (2 : 1), (b) LaF_3/CeO_2 (2 : 1), (c) LaF_3/CeO_2 (4 : 1), (d) LaF_3/ThO_2 (2 : 1).

the oxygen desorption is similar to that on LaF_3/CeO_2 (2 : 1). But besides the strong desorption from 41 to 242°C, there is still a weak desorption from 323 to 800°C. Among the oxygen species which desorbed, the strong desorption from 41 to 242°C might be O_2^- ions, while the weak desorption from 323 to 800°C might be O_2^{2-} or O^- species. These results are in agreement with the Raman result of LaF_3/CeO_2 (4 : 1).

Fig. 4d shows the TPD spectrum of oxygen species over LaF_3/ThO_2 (2 : 1). On LaF_3/ThO_2 (2 : 1), the oxygen desorption can be divided into three temperature regions, 35–270°C, 342–718°C and above 718°C. The desorption of 35–270°C might be the desorption of O_2^- ions [18]. 342–718°C might be the desorption of O_2^{2-} ions and unidentified intermediate oxygen species. The desorption above 718°C might be the desorption of O^- ions or part of O^{2-} ions. From the results, we see that the oxygen species on ThO_2/LaF_3 catalysts are much more complex than those on ZrO_2/LaF_3 and CeO_2/LaF_3 catalysts. The Raman spectra of LaF_3/ThO_2 (2 : 1) and LaF_3/ThO_2 (4 : 1) also revealed this fact.

From the above spectroscopic characterization of oxygen species on catalysts, on O_2 adsorbed LaF_3/ZrO_2 (2 : 1), the main active oxygen species were O_2^{2-} ions. For O_2 adsorbed LaF_3/CeO_2 (2 : 1) and LaF_3/CeO_2 (4 : 1), O_2^- ions are the main active oxygen species. O_2^{2-} ions are the next active oxygen species, but their amount is much less than that of O_2^- ions, and the amount of O_2^{2-} ions on LaF_3/CeO_2 (4 : 1) is larger than that on LaF_3/CeO_2 (2 : 1) (see Raman spectra and TPD). The kinds of active oxygen species found on O_2 adsorbed LaF_3/ThO_2 (2 : 1) and

LaF_3/ThO_2 (4 : 1) are the most numerous. Besides O_2^{2-}, O_2^- and O^- ions, there might be some unidentified intermediate active oxygen species ($O_2^{\delta-}$ $1<\delta<2$ or $0<\delta<1$). From the Raman and TPD of LaF_3/ThO_2 (2 : 1) and LaF_3/ThO_2 (4 : 1), we can find that the concentrations of active oxygen species on LaF_3/ThO_2 (2 : 1) and LaF_3/ThO_2 (4 : 1) were the highest.

4. Conclusion

The investigation indicated that, after LaF_3 was added to ZrO_2, CeO_2 or ThO_2 in the preparation process of catalysts, the $O^{2} \leftrightarrow F^-$ exchange between lattices might produce O^- ions or anion vacancies (one O^{2-} can substitute two F^-, then producing one anion vacancy), which are favourable for the activation of O_2, making the catalysts have high activity at low temperature.

Different metal oxides modified by LaF_3 might produce different kinds of active oxygen species, making the catalysts have different C_2 selectivities. The kinds and amounts of active oxygen species on LaF_3/ZrO_2 (2 : 1), LaF_3/CeO_2 (2 : 1) and LaF_3/CeO_2 (4 : 1) were less than those on LaF_3/ThO_2 (2 : 1) and LaF_3/ThO_2 (4 : 1). The C_2 selectivities of LaF_3/ZrO_2 (2 : 1), LaF_3/CeO_2 (2 : 1) and LaF_3/CeO_2 (4 : 1) were higher than those of LaF_3/ThO_2 (2 : 1) and LaF_3/ThO_2 (4 : 1). This might be caused by some kinds of active oxygen species on LaF_3/ThO_2 (2 : 1) and LaF_3/ThO_2 (4 : 1), which were favourable for the complete oxidation of hydrocarbons.

Acknowledgement

XRD and Raman spectra were measured in the State Key Laboratory for Physical Chemistry of the Solid Surface, Xiamen University. The support is gratefully acknowledged.

References

[1] G.E. Keller and M.M. Bhasin, J. Catal. 73 (1982) 9.
[2] S.J. Conway, D.J. Wang and J.H. Lunsford, Appl. Catal. 79 (1991) L1–L5.
[3] J.G. McCarty, M.A. Quinlan et al., ACS Div. Fuel. Chem. Preps. 33 (1988) 363.
[4] K. Aika et al., J. Chem. Soc. Chem. Commun. (1986) 1210.
[5] K. Otsuka and T. Komatsu, J. Chem. Commun. (1987) 388.
[6] X.D. Peng and P.C. Stair, J. Catal. 128 (1991) 264.
[7] A. Metcalfe and S. Udesgankar, J. Chem. Soc. Faraday Trans. I 76 (1980) 630.
[8] J.L. Gland, B.A. Sexton and G.B. Fisher, Surf. Sci. 95 (1980) 587.
[9] B.A. Sexton and R.J. Madix, Chem. Phys. Lett. 76 (1980) 294.
[10] C. Backx, P.P.M. Groot and P. Biloen, Surf. Sci. 104, (1981) 300.
[11] J.L. Gland, B.A. Sexton and B. Fisher, Surf. Sci. 95 (1980) 587.

[12] R. Imbihil and J.E. Demuth, Surf. Sci. 173 (1986) 395.
[13] G.W. Graham, W.H. Weber, C.R. Peters and R. Usmen, J. Catal. 130 (1991) 306.
[14] D. McIntosh and G.A. Ozin, Inorg. Chem. 16 (1977) 59.
[15] L. Andrews, J. Chem. Phys. 54 (1971) 4935;
D.A. Hatzenbuhler and L. Andrews, J. Chem. Phys. 56 (1972) 3398;
L. Andrews, J.T. Wang and C. Trindle, J. Phys. Chem. 77 (1973) 1065;
[16] F.J. Blunt, P.J. Hendra and J.R. Mackenzie, J. Chem. Soc. Chem. Commun. (1969) 278.
[17] F. Al-Mashta, N. Sheppard, V. Lorenzelli and G. Busca, J. Chem. Soc. Faraday Trans. I 78 (1982) 78.
[18] A.A. Davydov et al., Kinet. Katal. 10 (1969) 1125.
[19] A.B.P. Lever et al., Inorg. Chem. 19 (1980) 1823.
[20] J.S. Velentine, Chem. Rev. 73 (1973) 73.
[21] T. Ito, M. Yoshioka and T. Tokuda, J. Chem. Soc. Faraday Trans. I 79 (1983) 2277.
[22] T. Ito et al., J. Chem. Soc. Faraday Trans. I (1985) 2835.
[23] D. Cordischi et al., J. Chem. Soc. Faraday Trans. I 74 (1978) 456.